Experimental Hematology

Experimental Hematology 2019;74:42–51

Acute myeloid leukemia driven by the CALM-AF10 fusion gene is dependent on BMI1

Karina Barbosa[a], Anagha Deshpande[a], Bo-Rui Chen[a], Anwesha Ghosh[a], Younguk Sun[a], Sayantanee Dutta[b], Marla Weetall[c], Jesse Dixon[d], Scott A. Armstrong[e,f], Stefan K. Bohlander[g], and Aniruddha J. Deshpande[a]

[a]*Tumor Initiation and Maintenance Program, National Cancer Institute-Designated Cancer Center, Sanford Burnham Prebys Medical Discovery Institute, La Jolla, CA;* [b]*Department of Medicine III, University Hospital, LMU Munich, Munich, Germany;* [c]*PTC Therapeutics, South Plainfield, NJ;* [d]*Peptide Biology Laboratory, Salk Institute for Biological Studies, La Jolla, CA;* [e]*Department of Pediatric Oncology, Dana-Farber Cancer Institute, Boston, MA;* [f]*Division of Hematology/Oncology, Boston Children's Hospital, Harvard Medical School, Boston, MA;* [g]*Department of Molecular Medicine and Pathology, Faculty of Medical and Health Sciences, The University of Auckland, Auckland, New Zealand*

(Received 18 January 2019; revised 12 April 2019; accepted 15 April 2019)

A subset of acute myeloid and lymphoid leukemia cases harbor a t(10;11)(p13;q14) translocation resulting in the CALM-AF10 fusion gene. Standard chemotherapeutic strategies are often ineffective in treating patients with CALM-AF10 fusions. Hence, there is an urgent need to identify molecular pathways dysregulated in CALM-AF10-positive leukemias which may lay the foundation for novel targeted therapies. Here we demonstrate that the Polycomb Repressive Complex 1 gene *BMI1* is consistently overexpressed in adult and pediatric CALM-AF10-positive leukemias. We demonstrate that genetic *Bmi1* depletion abrogates CALM-AF10-mediated transformation of murine hematopoietic stem and progenitor cells (HSPCs). Furthermore, CALM-AF10-positive murine and human AML cells are sensitive to the small-molecule BMI1 inhibitor PTC-209 as well as to PTC-596, a compound in clinical development that has been shown to result in downstream degradation of BMI1 protein. PTC-596 significantly prolongs survival of mice injected with a human CALM-AF10 cell line in a xenograft assay. In summary, these results validate BMI1 as a bona fide candidate for therapeutic targeting in AML with CALM-AF10 rearrangements. © 2019 Published by Elsevier Inc. on behalf of ISEH – Society for Hematology and Stem Cells.

Acute leukemia patients often harbor genomic translocation events that give rise to oncogenic fusion proteins [1,2]. The t(10;11)(p13;q14) translocation is a recurrent, balanced translocation observed in human leukemia, which gives rise to the CALM-AF10 fusion protein [3,4]. Patients harboring the CALM-AF10 fusion have a particularly poor prognosis [5,6]. Standard chemotherapeutic strategies are often not very effective in treating patients with CALM-AF10 fusions. Hence, there is an urgent need to identify molecular pathways dysregulated in CALM-AF10-positive leukemias, which may lay the foundation for novel targeted therapies.

The N'-terminal partner of the fusion, CALM/PICALM, is a ubiquitously expressed component of the clathrin-mediated endocytosis (CME) pathway [7]. Mutations in the murine *Picalm* gene are associated with defects in iron uptake and hematopoiesis [8]. CALM deletion in the hematopoietic system leads to severe deficiencies in endocytic vesicle formation, transferrin-mediated iron uptake, and erythropoiesis [9–11]. The C'-terminal fusion partner AF10 (MLLT10), on the other hand, is a PHD finger-containing chromatin reader protein that acts as a co-factor for the histone methyltransferase DOT1L [12,13]. AF10 binds to the N-terminal histone H3 tail, with a preference for unmethylated lysine 27 (H3K27) [12]. Methylation of H3K27 strikingly lowers the affinity of the N-terminal chromatin-reading PHD–zinc knuckle–PHD module (PZP) of AF10 for chromatin [12]. Therefore, AF10 preferentially localizes to active chromatin domains where there are no repressive H3K27 methylation marks.

KB, AD, BC, YS, and AG performed experiments, analyzed data, and participated in manuscript preparation. AJD, SD, JD, SAA, MW, and SKB participated in data analysis, expert advice, and overall experimental design or contributed critical reagents. SKB and AJD conceptualized the project, designed experiments, and assisted in manuscript preparation.

Offprint requests to: Stefan K. Bohlander, Department of Molecular Medicine and Pathology, Faculty of Medical and Health Sciences, The University of Auckland, Auckland, New Zealand; E-mail: s.bohlander@auckland.ac.nz and Aniruddha J. Deshpande, 10901 North Torrey Pines Road, La Jolla, CA 92037; E-mail: adeshpande@sbpdiscovery.org

0301-472X/© 2019 Published by Elsevier Inc. on behalf of ISEH – Society for Hematology and Stem Cells.
https://doi.org/10.1016/j.exphem.2019.04.003

Early clues regarding the oncogenic mechanisms of CALM-AF10 came from transcriptome profiling studies using microarrays in acute myeloid leukemia (AML) and T-acute lymphoblastic leukemia (T-ALL). These studies indicated that CALM-AF10-rearranged leukemias have a distinct gene expression signature [14,15]. This signature resembles the transcriptome of leukemia cells with rearrangements of the mixed-lineage leukemia (MLL) gene in terms of elevated expression of the posterior *HOXA* genes and the TALE-domain co-factor *MEIS1*. One striking difference between CALM-AF10-rearranged and MLL-rearranged AMLs was the consistently elevated expression of *BMI1* in CALM-AF10-rearranged cases. Elevated *BMI1* expression is observed in AML as well as T-ALL with CALM-AF10 rearrangements [14,15].

BMI1 is a member of the Polycomb Repressive Complex 1 (PRC1) with critical roles in the repression of developmentally important genes, including genes involved in the self-renewal of somatic stem cells [16,17]. The most well-documented role of *Bmi1* is in the epigenetic repression of the *Ink4a* locus genes $p16^{Ink4a}$ and $p19^{Arf}$. This repressive activity of BMI1 is critical for its role in regulating cell-cycle progression and self-renewal of stem cells (reviewed in Park et al. [16] and Schuringa and Vellenga [17]). BMI1 mediates this repressive activity on chromatin by stimulating the enzymatic activity of the PRC1 RNF2/RING2 E3 ligase [18]. RNF2/RING2, the enzymatic component of the PRC1 complex, is responsible for the mono-ubiquitination of histone 2A at lysine 119 (H2AK119ub) leading to the epigenetic silencing of transcripts from H2AK119 mono-ubiquitinylated promoters [18–20].

High BMI1 expression is linked to oncogenic self-renewal in several tumors (reviewed in Park et al. [16] and Schuringa and Vellenga [17]). BMI1 overexpression is also implicated in epithelial-to-mesenchymal transition (EMT), metastasis, and chemotherapy resistance in solid tumors [21], marking this gene as an attractive therapeutic target in several human malignancies.

In this study, we investigated the role of BMI1 in CALM-AF10-rearranged AML using genetic and pharmacological approaches. Our results, using mouse and human models, reveal that genetic or pharmacological BMI1 inhibition impairs CALM-AF10-mediated leukemogenesis in vitro and in vivo.

Methods

Reagents

PTC-209 was obtained from Cayman Chemical Company (Ann Arbor, MI, USA), dissolved in dimethyl sulfoxide (DMSO), and stored at −80°C. PTC-596 and its vehicle solution for in vivo studies were provided by PTC Therapeutics (South Plainfield, NJ, USA).

Animal experiments

Bmi1-green fluorescent protein (GFP) transgenic mice (BKa.Cg-*Ptprc*^{b} *Bmi1*^{tm1Ilw} *Thy1*^{a}/J) mice were obtained from The Jackson Laboratories (Bar Harbor, ME, USA, JAX No. 017351) and maintained in the SBP animal facility. *Bmi1*$^{fl/fl}$ [22] mice were also obtained from The Jackson Laboratories (JAX No. 028974). All experiments using mice were conducted as per procedures approved by the SBP Institutional Animal Ethics Committee.

Cell culture

The human AML cell line U937 was a kind gift of Daniel Tenen, Beth Israel Deaconess Medical Center. The P31/Fujioka cells were obtained from the JCRB cell bank (No. JCRB0091). KP-MO-TS was a kind gift from Dr. Issay Kitabayashi, National Cancer Center, Tokyo. All cell lines were cultured in RPMI-1640 (Gibco, Grand Island, NY, USA) medium supplemented with 10% heat-inactivated fetal bovine serum (FBS), 2 mmol/L L-glutamine (Gibco), and 100 U/mL penicillin/streptomycin (Gibco). Murine bone marrow cells from the femur and tibia were depleted of lineage-positive cells using the EasySep Mouse Hematopoietic Progenitor Cell Isolation Kit (No. 19856, Stem-Cell Techologies, Vancouver, BC, Canada) and cultured overnight in Dulbecco's modified Eagle's medium (DMEM, Gibco) supplemented with 15% FBS (Gibco), 2 mM L-glutamine (Gibco), 100 U/mL penicillin/streptomycin (Gibco), and a cytokine cocktail containing mIL3, mIL6, and mSCF (Peprotech Inc). The following day, the cells were transduced with a retrovirally encoded version of CALM-AF10 bearing the C-terminal clathrin-binding domain of CALM and the octapeptide motif-leucine-zipper of AF10, as described in [23]. These bone marrow progenitors transduced with the CALM-AF10 fusion were then either used directly for experiments or injected into mice. For experiments involving Cre-mediated excision of *Bmi1*, murine leukemias bearing the Bmi1$^{fl/fl}$ background were transduced with viral particles encoding retrovirally expressed ER-Cre (in proliferation, apotosis and cell cycle assays) or Cre (in colony formation assays), with puromycin resistance transgenes for selection. For ER-Cre experiments, transduced Bmi1$^{fl/fl}$ cells were treated with puromycin after 2 days (2.5 μg/μL), for 3 days to generate stably expressing ER-Cre. Cells were treated with either DMSO as vehicle control or 100 nmol/L 4-hydroxytamoxifen (4-OHT) at the start of each assay. For experiments with constitutive retrovirally expressed Cre, Bmi1$^{fl/fl}$ cells were transduced, and 2 days later puromycin was added (2.5 μg/μL) to achieve selection of the transgene. Assays were started 3 days after puromycin treatment.

In vivo drug experiment

The xenograft model was established with NRG/SRM3 mice obtained from the SBP Animal Facility. Mice were irradiated (2.5 Gy), and 2×10^5 P31/Fujioka cells were then injected intravenously. At 9 days post-injection, engraftment of P31/Fujioka cells in NRG/SRM3 mice was confirmed by flow cytometric assessment of peripheral blood. (defined as ~1% human CD45+ cells), and mice were randomly assigned to two groups (n = 5) to receive either PTC-596 (12.5 mg/kg) or vehicle (0.5% hydroxypropyl methylcellulose and 0.1% Tween 80 in distilled water) by oral gavage twice per week. Circulating leukemia cells were detected on day 18 by flow

cytometry using a human-specific CD45 antibody (No. 404012, BioLegend, San Diego, CA). Retro-orbital bleedings were performed 18 days after tail vein injections of P31 cells and 10 days after initial dosing of PTC-596 or vehicle control. Red blood cells were lysed using 1 × PharmLyse Buffer (BD Biosciences), then washed with 1 × phosphate-buffered saline (PBS) and stained with APC-conjugated anti-human CD45 antibody (No. 404012, BioLegend) for 30 minutes in the dark, on ice. Cells were then washed again with 1 × PBS and analyzed on the LSR Fortessa. Mice were sacrificed upon signs of morbidity resulting from leukemic engraftment (>10% weight loss, lethargy, and ruffled fur).

Embryo generation and isolation of fetal liver cells

Embryos were generated from timed matings between male and female BKa.Cg-Ptprcb Bmi1tm1Ilw Thy1a/J mice. Detection of the vaginal plug was designated as E0.5. Pregnant females were sacrificed by cervical dislocation at E14.5. The uterine horns were removed, and fetuses were separated from maternal tissue. Fetal livers were dissected, and single-cell suspensions were obtained by straining tissues through a 10-μm mesh. Red blood cell (RBC) lysis was performed using 1 × RBC Lysis Buffer (Sigma-Aldrich, St. Louis, MO) according to the manufacturer's guidelines. Fetal liver cells were cultured in DMEM containing 15% FBS, 2 mmol/L L-glutamine (Gibco), 100 U/mL penicillin/streptomycin (Gibco), and a cytokine cocktail (mIL6, mIL3 and mSCF from Peprotech Inc., Rocky Hill, NJ, Nos. 216-16, 213-13, and 250-03).

Cell proliferation assays

Mouse and human (U937, P31/Fujioka and KP-MO-TS) CALM-AF10 cell lines were seeded and treated with DMSO (control) or PTC-209 (1 or 5 μmol/L). Samples were taken on the second, fourth, and sixth days after setup of the assay. Cell viability on treatment with PTC-209 was determined by using Sytox Blue Dead Cell Stain (Invitrogen) via flow cytometry. Analysis was performed on an LSR Fortessa (BD Biosciences). To estimate the EC_{50} of PTC-209, human cell lines U937 and P31 were seeded in a 384-well white square plate at a density of 1000 cells per well and treated with PTC-209 in a range of concentrations. Cells were counted after 2 days of treatment using the ATPlite 1step Luminescence Assay System in the EnVision microplate reader (Perkin Elmer, Waltham, MA) at the Conrad Prebys Center for Chemical Genomics (La Jolla, CA). Mouse CALM-AF10 cells were seeded in a 96-well plate at a density of 10,000 cells per well and treated with PTC-209. Cells were counted by FACS after 2 days of treatment, and viability was assessed by Sytox Blue staining. Both experiments were performed in three technical replicates. EC_{50} values were estimated using the Quest Graph IC50 Calculator (AAT Bioquest, Inc.) [24].

Cell cycle and apoptosis assay

Apoptosis induction was determined by combined Annexin V and Sytox staining. CALM-AF10 cell lines were treated with either DMSO or PTC-209 at 2.5 μmol/L. After 48 hours, cells were harvested and stained with Annexin V-APC (No. 550474, BD Pharmingen) for 15 minutes on ice in the dark. The cells were washed and stained with Sytox Blue Dead Cell Stain (Invitrogen, Thermo Fisher Scientific) before performing analysis. Cell cycle assessment was performed after 20 min of labeling with a BrdU-APC Flow kit (No. 552598, BD Pharmingen), according to the manufacturer's guidelines. All flow cytometric analyses were performed on an LSR Fortessa (BD Biosciences).

Colony formation assay

Mouse CALM-AF10 cell lines either treated or not treated with PTC-209 at 1 or 2.5 μmol/L were plated in duplicate in 1.1 mL methylcellulose-based medium (MethoCult 3234, StemCell Techologies) per well, containing 460 pmol/L mIL6, 1090 pmol/L mSCF, and 662 pmol/L mIL3 (Peprotech Inc) and incubated for 7 days. At the end of the incubation period, the numbers of blast and differentiated colonies were scored using an inverted microscope. Because almost all colonies were either compact or hypercellular (blast-like) or small and diffuse (consistent with differentiation), colonies were classified into these two categories [25].

Quantitative RT-PCR

Total RNA was isolated using TRIzol (No. 15596026, Thermo Fisher Scientific, San Jose, CA, USA) according to the manufacturer's instructions. cDNA was synthesized from extracted RNA using the ProtoScript First Strand cDNA Synthesis Kit (No. E6300, New England Biolabs Inc., Beverly, MA). Expression levels of human CDKN1A and ACTB, as well as mouse Cdkn2a and ActB, were measured using quantitative real-time reverse transcription polymerase chain reaction (RT-PCR using TaqMan Universal PCR Master Mix and pre-designed TaqMan gene expression assays (Applied Biosystems, Foster City, CA) on the Stratagene MX3000P (Agilent Technologies). Messenger RNA fold-change values were calculated in the basis of human ACTB or mouse ActB expression.

Statistical analysis

Flow cytometry data were analyzed using FlowJo (FlowJo Software, Tree Star, Ashland, OR). All statistical analyses were performed using GraphPad Prism 7 Software (San Diego, CA, USA), except for violin plots and their analysis, for which the R Statistical Software was used. p Values were calculated using Student's t test and two-way analysis of variance (ANOVA). In all figures, p values are summarized as $^{*}p < 0.05$, $^{**}p < 0.01$, $^{***}p < 0.001$, and $^{****}p < 0.0001$.

Results

Genetic Bmi1 *deletion impedes CALM-AF10-driven myeloid transformation*

We analyzed *BMI1* expression in RNA sequencing data from leukemia patients in The Cancer Genome Atlas (TCGA, http://cancergenome.nih.gov/) as well as the recently reported pediatric pan-cancer genome alteration studies [26]. We observed that patient samples with AF10 fusions, including both CALM-AF10 and MLL-AF10 fusions, expressed significantly higher levels of *BMI1* compared with non-AF10-rearranged samples. This was true for AML patients from TCGA studies (Figure 1A) as well as for childhood leukemia patients (AML, B-ALL,

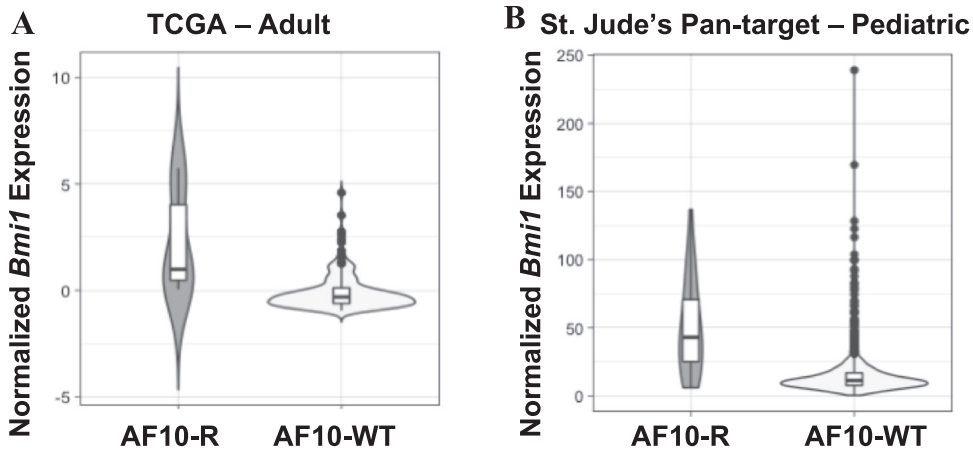

Figure 1. *BMI1* expression is plotted based on RNA-sequencing data sets from The Cancer Genome Atlas (TCGA LAML, left) or the Pediatric Cancer Data Portal (PeCan hematologic malignancies, right). Patients harboring AF10 rearrangements (AF10-R, $n = 6$ and $n = 27$) are compared with patients without AF10 rearrangements ($n = 167$ and $n = 1202$). p Value for PeCan comparison: 2e-16; for TCGA: 1.68e-5.

T-ALL, and mixed-lineage leukemia) from the pediatric pan-cancer studies [26] (Figure 1B). These observations indicate that *BMI1* may be directly activated by AF10-fusion oncogenes as suggested previously [27].

Given the high-level expression of *BMI1* in AF10 rearrangements, we wanted to investigate the potential requirement for BMI1 in CALM-AF10-driven AML. Towards this end, we utilized a well-established model of retroviral CALM-AF10 overexpression in murine hematopoietic stem and progenitor cells (HSPCs) [23]. First, we tested whether *Bmi1* deficiency can affect CALM-AF10-mediated oncogenic HSPC transformation. We obtained mice in which the *Bmi1* locus is replaced by the GFP transgene (termed BKa.Cg-*Ptprc*^{b} *Bmi1*^{tm1Ilw} *Thy1*^{a}/J mice). Because global *Bmi1* depletion leads to postnatal lethality in mice [28], we isolated fetal liver cells from day 14.5 mouse embryos that were heterozygous or homozygous for the *Bmi1 null* allele. We transduced these cells or their *Bmi1* wild-type counterparts with a retroviral expression vector encoding a highly oncogenic version of the CALM-AF10 fusion oncogene [23], along with a bicistronic TdTomato fluorescent reporter. TdTomato+ cells were sorted by fluorescence-assisted cell sorting (FACS) and plated for colony-forming unit (CFU) assays according to the scheme in Figure 2A). We observed that CALM-AF10 transduced cells showed a significant decrease in their ability to form undifferentiated, blast-like colonies (see Supplementary Figure E2), upon loss of *Bmi1* alleles, while differentiated colony formation was not significantly impaired (Figure 2B). These results indicate that Bmi1 is required for the immortalization of murine hematopoietic cells by the CALM-AF10 fusion gene. We then sought to determine whether hematopoietic cells already transformed by CALM-AF10 are also sensitive to *Bmi1* deletion. For this, we made use of another well-defined mouse with floxed *Bmi1* alleles (*Bmi1*$^{tm1.1Sjm}$/J), which would allow for conditional ablation of the *Bmi1* gene. We immortalized HSPCs from these *Bmi*$^{fl/fl}$ mice with the CALM-AF10 fusion gene. Subsequently, we transduced these rapidly growing cells with a retrovirally encoded estrogen receptor-fused Cre recombinase (ER-Cre) plasmid or a constitutive Cre recombinase. Treatment with 4-OHT induced Cre recombinase activity from the ER-Cre transduced cells, leading to excision of floxed *Bmi1* alleles (Figure 2C and data not shown). We then performed *in vitro* proliferation as well as CFU assays from CALM-AF10-transformed bone marrow cells treated with 4-OHT or vehicle control (DMSO). We observed that *Bmi1* deletion led to a significant and progressive decline in viable cell numbers compared with vehicle-treated cells (Figure 2D). This decrease in proliferation was accompanied by a significant increase in apoptotic cells as measured by Annexin V staining, as well as an increased ratio of cells in G0/G1 phase compared with S phase (Figure 2E). Using CFU assays, we also observed a significant decrease in the clonogenic capability of CALM-AF10-transformed cells upon *Bmi1* excision. Even though *Bmi1* deletion reduced the overall number of CFUs, the most striking reduction was observed in colonies with an undifferentiated or blast-like morphology (Figure 2F). Taken together, these experiments, using *Bmi1* constitutive or conditional knockout-mice, revealed that Bmi1 is critical for the initiation as well as maintenance of transformation by the CALM-AF10 fusion oncogene.

Small-molecule BMI1 inhibition impairs murine CALM-AF10 AML growth and survival

Recently, small molecule inhibitors of BMI1 have been developed [29,30]. We wanted to investigate whether these BMI1 inhibitors are active against CALM-AF10-driven AML. To do so, we utilized PTC-209, a novel

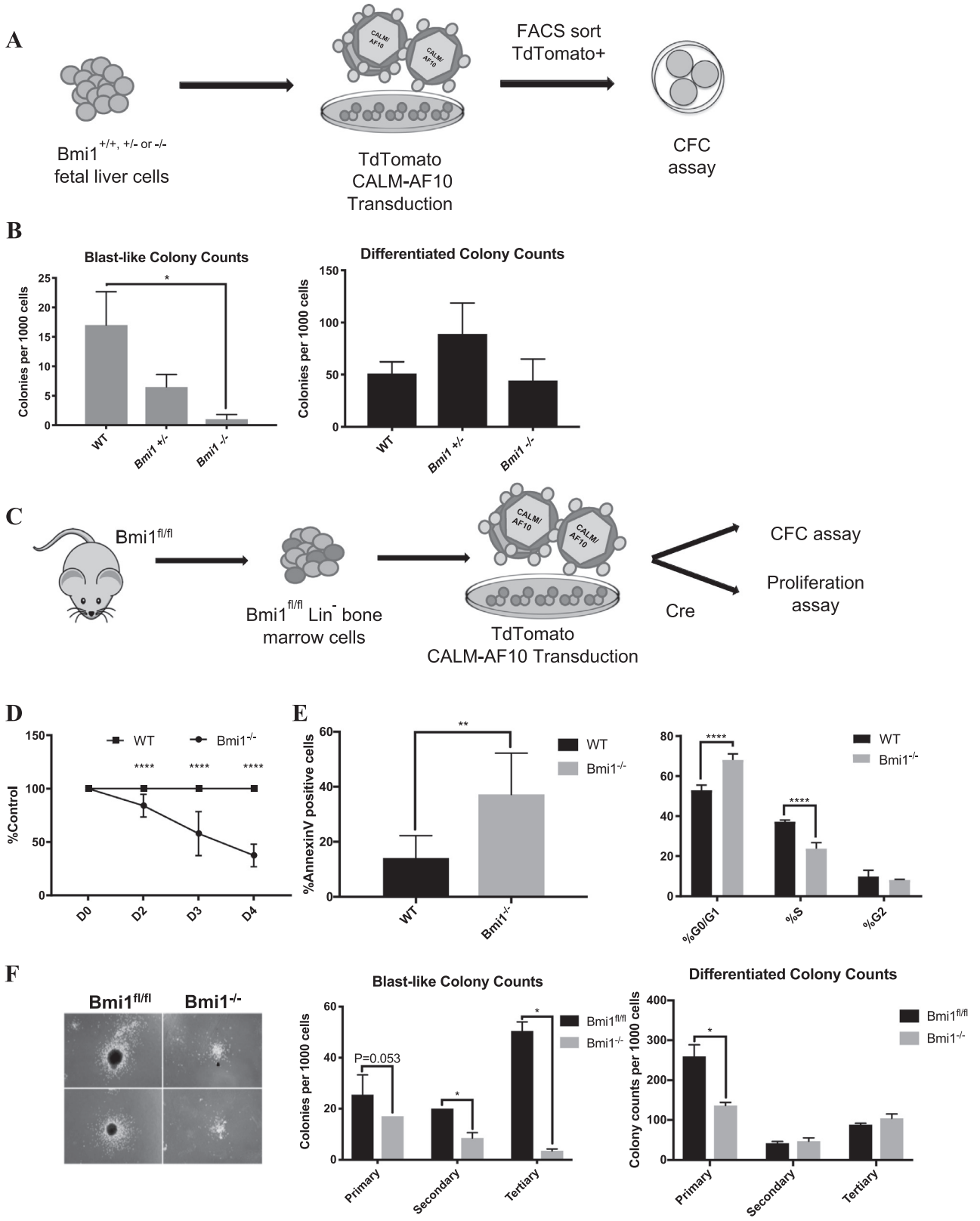

Figure 2. (A) Diagram illustrating the generation of retroviral CALM-AF10-transformed mouse cells with *Bmi1* wild-type or deficient backgrounds (fl/fl, fl/−, −/−). (B) Colony-forming units of CALM-AF10-transduced mouse fetal liver *Bmi1* mutant cells with blast-like (left) or differentiated (right) colonies at day 7. $*p < 0.05$, $n = 2$. (C) Diagram illustrating the generation of CALM-AF10-transformed mouse cells with $Bmi1^{fl/fl}$ backgrounds for *Bmi1* Cre-excision. (D) Analysis of *in vitro* cell proliferation of *Bmi1* excised mouse cells. $****p < 0.0001$, n=3. (E) Left: Annexin V staining in *Bmi1*-excised mouse cells. $**p < 0.0039$, $n = 3$. Right: Cell cycle progression analysis by propidium iodide staining in *Bmi1*-deleted mouse cells. $****p < 0.0001$, $n = 3$. (F) Representative images of colonies from CALM-AF10-transduced *Bmi1*-deleted and wild-type cells 1 week after plating. (I) Colony-forming units of CALM-AF10-transduced blast-like (left) or differentiated cells (right) at day 7. $*p < 0.05$, $n = 2$.

small molecule inhibitor of BMI1, previously used to target colorectal cancer, chronic leukemia, and multiple myeloma [31,32]. PTC-209 has been reported to reduce expression of BMI1 protein by altering regulation of the translation of the BMI1 mRNA [29]. We examined the effect of PTC-209 on mouse CALM-AF10 AML cell growth by treating primary AML cells from three independently derived tumors. Cells were exposed to varying concentrations of PTC-209 for up to 6 days together with DMSO-treated controls, and viable cells were counted every 2 days. First, we confirmed on-target activity of PTC-209 by ensuring the de-repression of the Cdkn2a locus, a well-characterized tumor suppressor locus that is transcriptionally repressed by Bmi1 activity (Supplementary Figure E1D, online only, available at www.exphem.org). We then assessed the effect of PTC-209 on CALM-AF10-transformed AML cells in proliferation assays *in vitro*. We observed that PTC-209 induced a highly significant and concentration-dependent decrease in the number of viable CALM-AF10 AML cells over time (Figure 3A) in comparison to their vehicle-treated counterparts. This decrease in cell viability was accompanied by a significant increase in Annexin V-positive cells, demonstrating induction of apoptosis 48 hours after PTC-209 treatment (Figure 3B). The sensitivity of CALM-AF10 AML cells to PTC-209 was in the low micromolar range with an EC_{50} of 1.9 μmol/L (Supplementary Figure E3, online only, available at www.exphem.org).

Furthermore, compared with vehicle-treated AML cells, PTC-209 treatment also significantly reduced the clonogenic capacity of CALM-AF10 cells in CFU assays in a concentration-dependent manner (Figure 3C, D). These results demonstrate that small-molecule BMI1 inhibitor significantly inhibits the proliferative activity as well as clonogenic capability of murine CALM-AF10 AML cells.

Pharmacological BMI1 inhibition impairs human CALM-AF10 AML in vitro and in vivo

We wanted to confirm our findings from the mouse models in human CALM-AF10-rearranged AML. For this, we treated the CALM-AF10-rearranged AML cell lines U937, KPMOTS, and P31/Fujioka *in vitro* with DMSO or PTC-209 at various concentrations and assessed the effect on proliferation, cell cycle, and apoptosis. In proliferation assays, we observed a significant and concentration-dependent decrease in viable cell counts of all three cell lines upon treatment with PTC-209, compared with DMSO controls (Figure 4A). After 48 h of treatment, PTC-209 also induced consistent increases in Annexin V-positive cell populations compared with the vehicle, with the most significant

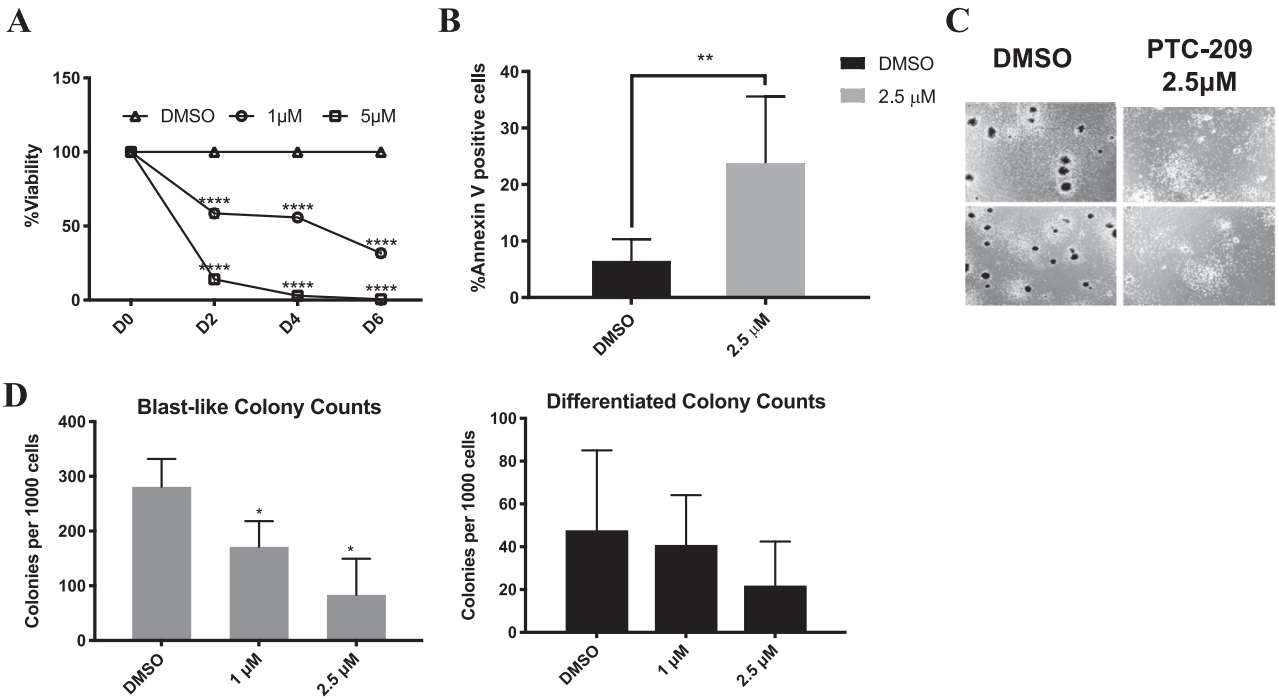

Figure 3. (A) Percentage of viable cells from mouse CALM-AF10-transformed AML cells upon PTC-209 treatment compared with DMSO-treated counterparts. *$p < 0.05$, $n = 9$. (B) Annexin V staining in mouse CALM-AF10-transformed cell lines. *$p < 0.05$, $n = 9$. (C) Representative images of colonies from mouse CALM-AF10-transformed cells upon 7 days of PTC-209 treatment. (D) Colony-forming units of CALM-AF10 immortalized mouse cells upon PTC-209 versus DMSO treatment. Blast (left) and differentiated (right) colonies at day 7. *$p < 0.05$, $n = 2$.

and most pronounced difference in P31/Fujioka cells (Figure 4B). Similar to mouse CALM-AF10-transformed cells, BrdU incorporation analysis showed an increase in the proportion of G0/G1 phase cells in U937, P31/Fujioka, and KPMOTS cell lines, with a corresponding decrease in S-phase cells (Figure 4C). Taken together, small-molecule BMI1 inhibition results in cell-cycle arrest features that are coupled with increased cell death and reduced proliferation of CALM-AF10-driven human AML cell lines, in concordance with our mouse model data.

Next, we wanted to validate our findings *in vivo*. For this, we used PTC-596, a compound in clinical development identified by its ability to inhibit proliferation of BMI1-positive cancer stem cells [30,33–35]. The mechanism underlying BMI1 protein reduction is thought to be to G2/M arrest causing accelerated ubiquitination and degradation of the BMI1 protein [36]. We assessed the ability of PTC-596 to inhibit CALM-AF10-driven *in vivo* leukemogenesis. First, we injected immunodeficient mice (NRG-SGM3) with the P31/Fujioka cell line. Ten days after injection, we confirmed engraftment of P31 cells in mice by flow cytometric assessment of the human CD45 marker (Supplementary Figure E3). We then orally administered PTC-596 to one cohort of mice and the vehicle control to an age- and engraftment-matched cohort. We observed that PTC-596 treatment significantly delayed the latency of disease in mice compared with controls (Figure 5; Supplementary Figure E4, online only, available at www.exphem.org), demonstrating the *in vivo* efficacy of small-molecule BMI targeting in this setting.

In summary, our results indicate that BMI1 is a bona fide candidate for therapeutic targeting in AML with CALM-AF10 rearrangements and possibly other leukemias with CALM-AF10 rearrangements.

Discussion

Despite the well-described oncogenic activity of BMI1 in a wide range of human cancers, therapeutic BMI1 targeting has proven to be elusive. Recently, the BMI1 small-molecule inhibitor PTC-209 was developed by PTC Therapeutics [29] and has been used in pre-clinical studies to treat chronic and acute myeloid leukemia [32], biliary tract cancer [31], multiple myeloma [37,38], non-small cell lung cancer [39], glioblastoma [40], ovarian cancer [41], prostate cancer [42], breast cancer [43], and colorectal cancer [29]. Furthermore, a next-generation clinical-grade BMI1 inhibitor, PTC-596, has been developed and is currently in clinical trials for advanced solid tumors [33]. The fact that elevated *BMI1* expression is a common feature of CALM-

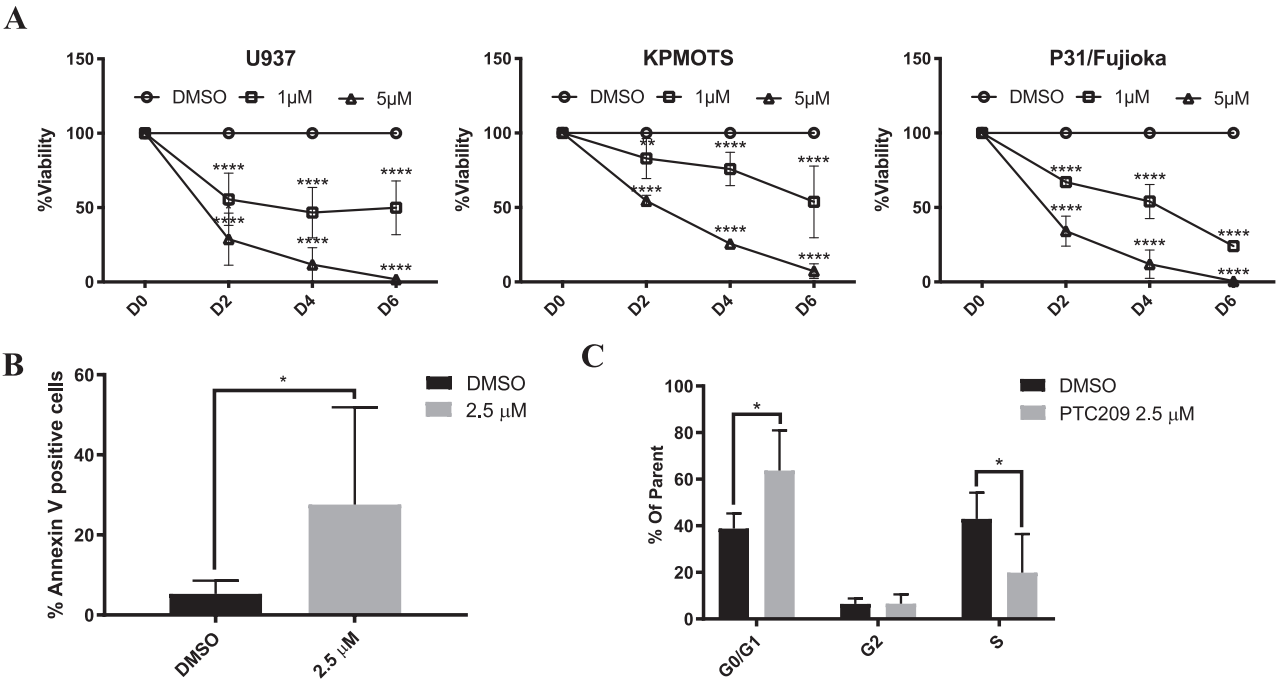

Figure 4. (A) Analysis of *in vitro* cell proliferation of human CALM-AF10-driven cell lines upon PTC-209 treatment. *$p < 0.05$, $n = 6$. (B) Annexin V staining in human CALM-AF10-driven cell lines. *$p < 0.05$, $n = 3$. (C) Cell cycle analysis by bromodeoxyuridine incorporation in human CALM-AF10-driven cell lines. *$p < 0.05$, $n = 3$.

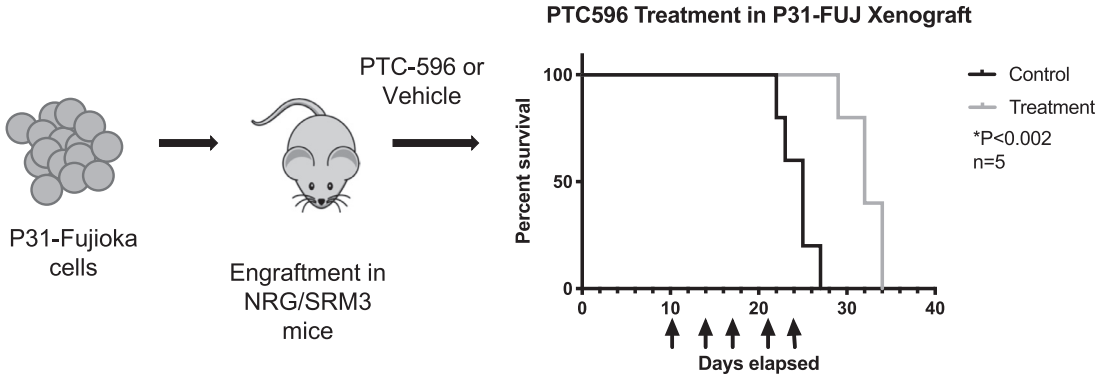

Figure 5. Diagram illustrating *in vivo* human CALM-AF10 cell line engraftment model and treatment with clinical-grade inhibitor PTC-596. On the right is the survival curve for PTC-596- versus vehicle-treated animals ($n = 5$ mice per group, $*p < 0.002$).

AF10 leukemias regardless of lineage suggests that BMI1 may be a transcriptional target of the CALM-AF10 fusion protein. Intriguingly, we have previously noted that BMI1 is located on chromosome 10 adjacent to and downstream of the wild-type AF10 gene [27]. Therefore, it is also likely that the CALM-AF10 fusion event drives enhanced BMI1 expression through the disruption of topologically associated domains (TADs) and juxtaposition of BMI1 to the strong, CALM-associated enhancers, as a result of the t(10;11) translocation. Because elevated *Bmi1* expression can be observed even in mouse models of CALM-AF10-driven AML [27], which do not harbor a t(10;11) translocation, the former scenario is more likely, although the latter possibility with TAD activation cannot completely be ruled out. Regardless of the mechanism of BMI1 activation, this characteristic CALM-AF10-associated molecular event may create a novel dependency that is therapeutically tractable.

The role of BMI1 in AML has been studied in the context of leukemias driven by other leukemia-associated oncogenes. Interestingly, genetic experiments revealed that the dependency on BMI1 is selective. Bmi1 was first reported to be important for AML stem cells in a murine study using a retroviral model of Hoxa9 and Meis1 co-expression [44]. This study showed that *Bmi1* deletion does not affect the initiation of Hoxa9–Meis1-driven AML, but significantly impairs the ability of primary leukemias to transmit disease in secondary recipients [44]. This study indicated that Bmi1 was important for the self-renewal of leukemia stem cells in the retroviral Hoxa9–Meis1 co-expression model. Other studies demonstrated that although myeloid transformation driven by the fusion oncoproteins AML1-ETO and PLZF-RARA is strongly sensitive to Bmi1 depletion [45,46], leukemias driven by the MLL-AF9 fusion oncoprotein are not dependent on *Bmi1* expression [46]. Another study with the MLL-AF9 fusion protein observed that *Bmi1* was necessary for the generation of AML from granulocyte macrophage progenitors (GMPs), indicating that BMI1 may be critical for leukemic transformation of downstream hematopoietic progenitors by MLL-AF9, but not for the transformation of hematopoietic stem cells (HSCs) [47]. These studies demonstrate the selective requirement of BMI1 depending on the mutational subtype of AML as well as on the developmental stage of the leukemia cells. In our studies, CALM-AF10-driven transformation seems to require Bmi1 for both the initiation of transformation and maintenance. More recently, the small-molecule BMI1 inhibitors PTC-209 and PTC-596 have been used to demonstrate that a broad panel of human AML cell lines are sensitive to small-molecule BMI1 inhibition [30,32,36], although none of these studies focused specifically on CALM-AF10-rearranged AML. In CALM-AF10, the clinical rationale for BMI1 targeting may be clearer, given that BMI1 is strongly upregulated in CALM-AF10 rearranged AML.

Our observation that CALM-AF10 fusions require BMI1 for initiation as well as maintenance of transformation provides pre-clinical evidence that pharmacological BMI1 inhibition may provide potential clinical benefit in leukemias with CALM-AF10 rearrangements. These results could help inform future clinical trials with BMI1 inhibitors. It is pertinent to note that BMI1 upregulation is observed not only in CALM-AF10-positive AML, but also in T-ALL, in which elevated BMI1 expression was first noted [14]. It is therefore very likely that small-molecule BMI1 inhibition is a lineage-independent vulnerability associated with CALM-AF10 rearrangements. The hypothesis that CALM-AF10-rearranged T-ALLs may also be sensitive to BMI1 inhibition needs to be validated using T-ALL models of this disease. Even though CALM-AF10 fusions are more frequent in T-ALL than in AML, CALM-AF10 mouse models reported so far are biased toward the myeloid lineage [23,48–50], hampering the

validation of therapeutic candidates for CALM-AF10-positive T-ALL. Future studies will focus on the development of CALM-AF10 T-ALL models and the validation of BMI1 inhibitors in these studies.

Acknowledgments

We acknowledge Yoav Altman and Amy Cortez at the SBP Flow cytometry core facility for sorting our samples and Buddy Charbono at the Animal Facility at SBP for mouse injections. We acknowledge the support of the Lady Tata Memorial Foundation to AD. We acknowledge our funding sources: NIH R00 CA154880, NIH/NCI P30 CA030199, as well as the ASH Scholar award and the V-Foundation Award to AJD. SKB was supported by Leukaemia and Blood Cancer New Zealand and the family of Marijana Kumerich.

Conflict of Interest Disclosure

AJD is a consultant at A2A Pharmaceuticals, New Jersey and Salgomed Therapeutics, La Jolla, California. MW is employed by PTC Therapeutics and has received salary and compensation for time, effort, and hold or held financial interest in the company.

References

1. Greaves MF, Wiemels J. Origins of chromosome translocations in childhood leukaemia. Nat Rev Cancer. 2003;3:639–649.
2. Rowley JD. The role of chromosome translocations in leukemogenesis. Semin Hematol. 1999;36(4, Suppl 7):59–72.
3. Bohlander SK, Muschinsky V, Schrader K, et al. Molecular analysis of the CALM/AF10 fusion: Identical rearrangements in acute myeloid leukemia, acute lymphoblastic leukemia and malignant lymphoma patients. Leukemia. 2000;14:93–99.
4. Caudell D, Aplan PD. The role of CALM-AF10 gene fusion in acute leukemia. Leukemia. 2008;22:678–685.
5. Dreyling MH, Schrader K, Fonatsch C, et al. MLL and CALM are fused to AF10 in morphologically distinct subsets of acute leukemia with translocation t(10;11): Both rearrangements are associated with a poor prognosis. Blood. 1998;91:4662–4667.
6. Narita M, Shimizu K, Hayashi Y, et al. Consistent detection of CALM-AF10 chimaeric transcripts in haematological malignancies with t(10;11)(p13;q14) and identification of novel transcripts. Br J Haematol. 1999;105. 41565431928−937.
7. Tebar F, Bohlander SK, Sorkin A. Clathrin assembly lymphoid myeloid leukemia (CALM) protein: Localization in endocytic-coated pits, interactions with clathrin, and the impact of overexpression on clathrin-mediated traffic. Mol Biol Cell. 1999;10:2687–2702.
8. Klebig ML, Wall MD, Potter MD, Rowe EL, Carpenter DA, Rinchik EM. Mutations in the clathrin-assembly gene *Picalm* are responsible for the hematopoietic and iron metabolism abnormalities in *fit1* mice. Proc Natl Acad Sci USA. 2003;100:8360–8365.
9. Ishikawa Y, Maeda M, Pasham M, et al. Role of the clathrin adaptor PICALM in normal hematopoiesis and polycythemia vera pathophysiology. Haematologica. 2015;100:439–451.
10. Scotland PB, Heath JL, Conway AE, et al. The PICALM protein plays a key role in iron homeostasis and cell proliferation. PLoS ONE. 2012;7(8):e44252.
11. Suzuki M, Tanaka H, Tanimura A, et al. The clathrin assembly protein PICALM is required for erythroid maturation and transferrin internalization in mice. PLoS ONE. 2012;7(2):e31854.
12. Chen S, Yang Z, Wilkinson AW, et al. The PZP domain of AF10 senses unmodified H3K27 to regulate DOT1L-mediated methylation of H3K79. Mol Cell. 2015;60:319–327.
13. Deshpande AJ, Deshpande A, Sinha AU, et al. AF10 regulates progressive H3K79 methylation and HOX gene expression in diverse AML subtypes. Cancer Cell. 2014;26:896–908.
14. Dik WA, Brahim W, Braun C, et al. CALM-AF10+ T-ALL expression profiles are characterized by overexpression of HOXA and BMI1 oncogenes. Leukemia. 2005;19:1948–1957.
15. Mulaw MA, Krause A, Riedel A, Tizazu B, Reuter H, Bohlander SK. Early target genes of CALM/AF10 as revealed by gene expression profiling. Blood. 2008;112:2260.
16. Park IK, Morrison SJ, Clarke MF. Bmi1, stem cells, and senescence regulation. J Clin Invest. 2004;113:175–179.
17. Schuringa JJ, Vellenga E. Role of the polycomb group gene BMI1 in normal and leukemic hematopoietic stem and progenitor cells. Curr Opin Hematol. 2010;17:294–299.
18. Cao R, Tsukada Y, Zhang Y. Role of Bmi-1 and Ring1A in H2A Ubiquitylation and Hox gene silencing. Mol Cell. 2005;20:845–854.
19. Buchwald G, Van Der Stoop P, Weichenrieder O, Perrakis A, Van Lohuizen M, Sixma TK. Structure and E3-ligase activity of the Ring-Ring complex of polycomb proteins Bmi1 and Ring1b. EMBO J. 2006;25:2465–2474.
20. Kallin EM, Cao R, Jothi R, et al. Genome-wide uH2A localization analysis highlights Bmi1-dependent deposition of the mark at repressed genes. PLoS Genet. 2009;5(6):e1000506.
21. Siddique HR, Saleem M. Concise review: Role of BMI1, a stem cell factor, in cancer recurrence and chemoresistance: Preclinical and clinical evidences. Stem Cells. 2012;30:372–378.
22. Mich JK, Signer RA, Nakada D, et al. Prospective identification of functionally distinct stem cells and neurosphere-initiating cells in adult mouse forebrain. ELife. 2014;3:e02669.
23. Deshpande AJ, Rouhi A, Lin Y, et al. The clathrin-binding domain of CALM and the OM-LZ domain of AF10 are sufficient to induce acute myeloid leukemia in mice. Leukemia. 2011;25:1718–1727.
24. AAT Bioquest, Inc. Quest Graph™ IC50 Calculator. Available at:https://www.aatbio.com/tools/ic50-calculator. Accessed: April 5, 2019.
25. Deshpande AJ, Chen L, Fazio M, et al. Leukemic transformation by the MLL-AF6 fusion oncogene requires the H3K79 methyltransferase Dot1l. Blood. 2013;121:2533–2541.
26. Ma X, Liu Y, Liu Y, et al. Pan-cancer genome and transcriptome analyses of 1,699 paediatric leukaemias and solid tumours. Nature. 2018;555:371–376.
27. Mulaw MA, Krause AJ, Deshpande, et al., et al. CALM/AF10-positive leukemias show upregulation of genes involved in chromatin assembly and DNA repair processes and of genes adjacent to the breakpoint at 10p12. Leukemia. 2012;26:1012–1019.
28. Park IK, Qian D, Kiel M, et al. Bmi-1 is required for maintenance of adult self-renewing haematopoietic stem cells. Nature. 2003;423:302–305.
29. Kreso A, van Galen P, Pedley NM, et al. Self-renewal as a therapeutic target in human colorectal cancer. Nat Med. 2014;20:29–36.
30. Nishida Y, Maeda A, Kim MJ, et al. The novel BMI-1 inhibitor PTC-596 downregulates MCL-1 and induces p53-independent mitochondrial apoptosis in acute myeloid leukemia progenitor cells. Blood Cancer J. 2017;7:e527.
31. Mayr C, Neureiter D, Wagner A, Pichler M, Kiesslich T. The role of polycomb repressive complexes in biliary tract cancer. Expert Opin Therap Targets. 2015;19:363–375.
32. Mourgues L, Imbert V, Nebout M, et al. The BMI1 polycomb protein represses cyclin G2-induced autophagy to support proliferation in chronic myeloid leukemia cells. Leukemia. 2015;29:1993–2002.

33. Infante JR, Bedard PL, Shapiro G, et al. Phase 1 results of PTC-596, a novel small molecule targeting cancer stem cells (CSCs) by reducing levels of BMI1 protein. J Clin Oncol. 2017;35(15, Suppl.). 2574–2574.
34. Maeda A, Nishida Y, Weetall M, et al. Targeting of BMI-1 expression by the novel small molecule PTC-596 in mantle cell lymphoma. Oncotarget. 2018;9:28547–28560.
35. Nishida Y, Maeda A, Cao L. et al. Targeting BMI-1 by the novel BMI-1 inhibitor PTC-209 in acute leukemia. Mol Cancer Therap. 2015;14(12, Suppl. 2):A130.
36. Sahasrabuddhe A A, Dimri M, Bommi P V, Dimri G P. βTrCP regulates BMI1 protein turnover via ubiquitination and degradation. Cell Cycle. 2011;10:1322–1330.
37. Bolomsky A, Heusschen R, Stangelberger K, et al. Preclinical evaluation of the first in class BMI1 inhibitor PTC-028 confirms potent efficacy to target BMI1-addiction in multiple myeloma. Blood. 2017;130:1804.
38. Bolomsky A, Schlangen K, Schreiner W, Zojer N, Ludwig H. Targeting of BMI-1 with PTC-209 shows potent anti-myeloma activity and impairs the tumour microenvironment. J Hematol Oncol. 2016;9:17.
39. Yong KJ, Basseres DS, Welner RS, et al. Targeted BMI1 inhibition impairs tumor growth in lung adenocarcinomas with low CEBPα expression. Sci Transl Med. 2016;8(350):350ra104.
40. Jin X, Kim LJY, Wu Q, et al. Targeting glioma stem cells through combined BMI1 and EZH2 inhibition. Nat Med. 2017;23:1352.
41. Dey A, Mustafi SB, Saha S, Kumar Dhar Dwivedi S, Mukherjee P, Bhattacharya R. Inhibition of BMI1 induces autophagy-mediated necroptosis. Autophagy. 2016;12:659–670.
42. Bansal N, Bartucci M, Yusuff S, et al. BMI-1 targeting interferes with patient-derived tumor-initiating cell survival and tumor growth in prostate cancer. Clin Cancer Res. 2016;22:6176–6191.
43. Dimri M, Kang M, Dimri GP, et al. A miR-200c/141-BMI1 autoregulatory loop regulates oncogenic activity of BMI1 in cancer cells. Oncotarget. 2016;7:36220–36234.
44. Lessard J, Sauvageau G. Bmi-1 determines the proliferative capacity of normal and leukaemic stem cells. Nature. 2003;423:255–260.
45. Boukarabila H, Saurin AJ, Batsché E, et al. The PRC1 Polycomb group complex interacts with PLZF/RARA to mediate leukemic transformation. Genes Dev. 2009;23:1195–1206.
46. Smith LL, Yeung J, Zeisig BB, et al. Functional crosstalk between Bmi1 and MLL/Hoxa9 axis in establishment of normal hematopoietic and leukemic stem cells. Cell Stem Cell. 2011;8:649–662.
47. Yuan J, Takeuchi M, Negishi M, Oguro H, Ichikawa H, Iwama A. Bmi1 is essential for leukemic reprogramming of myeloid progenitor cells. Leukemia. 2011;25:1335–1343.
48. Caudell D, Zhang Z, Yang JC, Aplan PD. Expression of a CALM-AF10 fusion gene leads to Hoxa cluster overexpression and acute leukemia in transgenic mice. Cancer Res. 2007;67:8022–8031.
49. Deshpande AJ, Cusan M, Rawat VPS, et al. Acute myeloid leukemia is propagated by a leukemic stem cell with lymphoid characteristics in a mouse model of CALM/AF10-positive leukemia. Cancer Cell. 2006;10:363–374.
50. Dutta S, Krause A, Vosberg S, et al. The target cell of transformation is distinct from the leukemia stem cell in murine CALM/AF10 leukemia models. Leukemia. 2016;30:1166–1176.

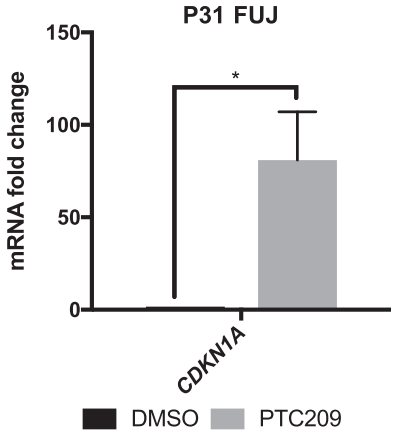

Supplementary Figure E1. Normalized mRNA fold-change values for human CDKN1A, measured by quantitative real-time reverse transcription polymerase chain reaction after 48 hours of PTC-209 treatment in P31/Fujioka cells. $*p < 0.05$, $n = 2$.

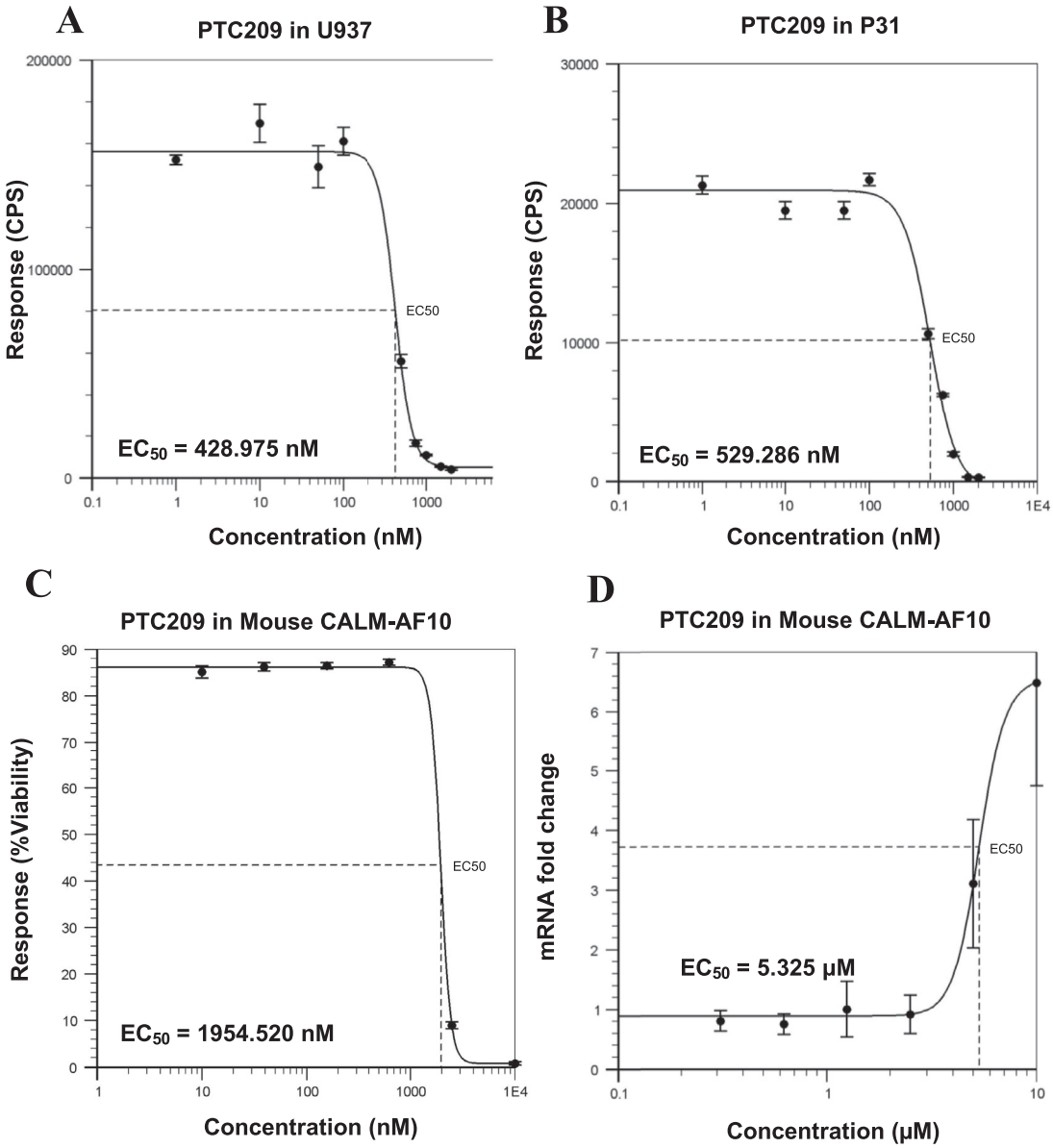

Supplementary Figure E2. PTC-209 EC_{50} estimation in CALM-AF10+ AML. (A) Counts per second (CPS) values for the human CALM-AF10 + cell lines U937 and (B) P31/Fujioka, shown on the *y*-axis, are the result of ATPlite measurements taken 48 hours after treatment with a range of PTC-209 concentrations. The EC_{50} calculated values are 428.975 and 529.286 nmol/L, respectively; $n = 3$ in both panels. (C) Viability responses of mouse CALM-AF10 cells estimated by flow cytometry after 48 hours of treatment with a range of PTC-209 concentrations (*x*-axis). $EC_{50} = 1954.520$ nmol/L, $n = 3$. (D). Normalized mRNA fold-change values for mouse Cdkn2a, measured by quantitative real-time reverse transcription polymerase chain reaction after 48 hours of PTC-209 treatment with a range of concentrations (0–10 μmol/liter) for an EC_{50} response estimation ($EC_{50} = 5.325$ μmol/liter). $^*p < 0.05$, $n = 3$.

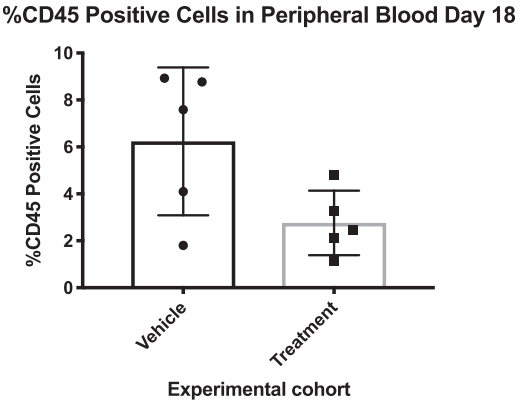

Supplementary Figure E3. Percentage of circulating P31/Fujioka cells in peripheral blood of NRG/SRM3 mice. Flow cytometric assessment of human CD45-stained cells as a percentage of live cells shown on the *y*-axis for both vehicle control ($n = 5$) and PTC-596 "treatment" ($n = 5$) groups, 18 days after intravenous injection of P31/Fujioka cells.

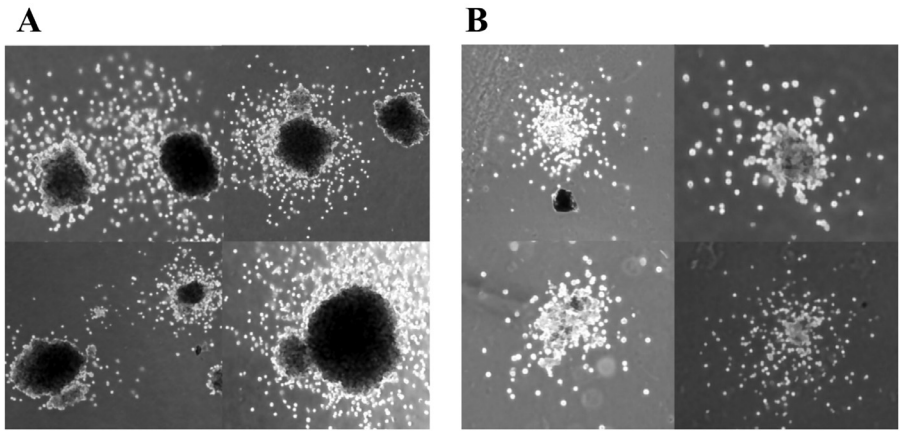

Supplementary Figure E4. Representative (A) compact or hypercellular blast-like and (B) small and diffuse differentiated colonies from colony-forming unit assays. Scoring across experiments was performed according to these examples, in agreement with previous studies [25].